Geophysical Journal International

Geophys. J. Int. (2014) **197,** 1107–1116
Advance Access publication 2014 February 25

doi: 10.1093/gji/ggu044

A new method for earthquake depth determination: stacking multiple-station autocorrelograms

Miao Zhang,[1] Dongdong Tian[1] and Lianxing Wen[2,1]

[1] *Laboratory of Seismology and Physics of Earth's Interior; School of Earth and Space Sciences, University of Science and Technology of China, Hefei, Anhui* 230026*, P. R. China. E-mail: zhmiao@mail.ustc.edu.cn*
[2] *Department of Geosciences, State University of New York at Stony Brook, Stony Brook, New York, USA*

Accepted 2014 February 3. Received 2014 January 23; in original form 2013 October 18

SUMMARY

Accurate determination of earthquake depth is important, but particularly challenging. We develop a new method to determine the earthquake source depth by stacking multiple-station autocorrelograms (SMAC) of seismic data. The basic concept of SMAC method is to enhance the coherent surface reflected energy by autocorrelation and stacking, and uses the surface reflected energy to determine the source depth. Autocorrelation effectively enhances the energy of the seismic phases related to the source depth, while stacking the autocorrelograms of array data further improves the signal-to-noise ratio of the energy. The procedures are applied using both the main *SH* waves and the coda. Using coda waves, the method extracts the two-way traveltime between the source and the surface by stacking the coda wave autocorrelations over an array of seismic observations. Using the main *SH* waves, SMAC explores the interference of the down-going Moho reflected *SmS* wave and up-going surface bounced Moho reflected *sSmS* wave by autocorrelation. The autocorrelograms are then stacked along theoretical differential *sSmS–SmS* traveltime predicted for all potential source depths, and the source depth is determined to be the one that produces the maximum stacking energy. Synthetic tests demonstrate the validity of the SMAC procedures. As an example of application, we apply the SMAC method to determine the source depth of an earthquake occurring in Japan Island. The procedures of using both main *SH* waves and their coda waves yield robust surface reflected energy and a consistent source depth. The error of the depth estimation is less than 1 km assuming an uncertainty of 10 per cent in the averaged crust velocity.

Key words: Interferometry; Earthquake source observations; Wave scattering and diffraction; Wave propagation.

1 INTRODUCTION

Accurate determination of earthquake location is important for better understanding earthquake physics, Earth's internal structure and temporal change of medium, etc. The accuracy of our determination of absolute hypocentre location would depend on many factors, including seismic coverage, accuracy of arrival-time picking and our knowledge of crustal structure (e.g. Pavlis 1986). While modern relocation methods using differential traveltime between earthquakes significantly improve the accuracy of event relocation (Poupinet *et al.* 1984; Waldhauser & Ellsworth 2000; Schaff & Richards 2004; Lin & Shearer 2005; Shearer *et al.* 2005; Wen 2006), these relocation results still depend on the accuracy of the input initial absolute event locations. In locating the absolute event position, the determination of source depth of a crustal earthquake is of particularly challenging, because of indiscernible depth phases from those earthquakes and strong trade-off between source depth and event origin time in relocation (e.g. Billings *et al.* 1994).

While identifying depth phase of a seismic event would provide the most reliable information for determining the source depth (King 1979; Zonno & Kind 1984; Langston 1987), it is not discernable in the recorded seismograms because of strong underground scattering. In this paper, we develop a method to determine earthquake source depth by stacking multiple-station autocorrelograms (SMAC) of main *SH* waves and their coda waves. The method enhances the coherent surface reflected energy by autocorrelation and stacking, and uses the surface reflected energy to determine the source depth. We introduce the theory of the method and demonstrate its validity using synthetics in Sections 2 and 3, apply the method to determine the source depth of an earthquake occurring in Japan Island in Section 4 and discuss possible implications of the method in Section 5.

2 THEORETICAL FRAMEWORK OF SMAC

In this study, we present the theoretical framework of the method in the case of *SH* wave propagation. The theoretical framework in the *P-SV* system can be derived in a similar way, but would not be dealt

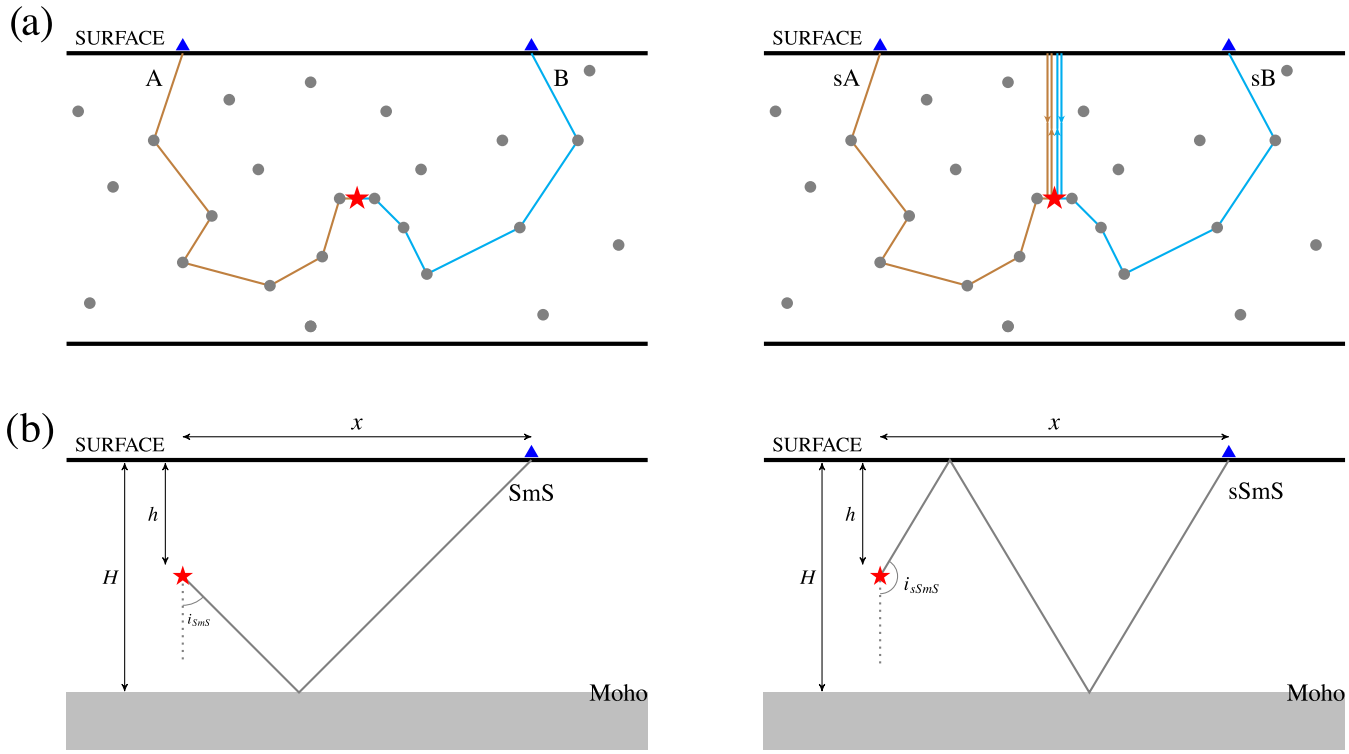

Figure 1. (a) Cartoon illustrating the concept of SMAC method for depth determination using coda waves. The method utilizes the interference of the scattered waves (two example paths A, B on the left panel) and the surface reflected scattered waves with otherwise same scattering paths (two example counterpart paths sA, sB on the right panel) in the autocorrelograms. The energy pairs of A, sA and B, sB would both appear at the two-way traveltime between source and the surface in their autocorrelograms, and are enhanced by stacking over many stations. Earthquake, seismic stations and seismic scatterers are represented by red star, blue triangles and grey points, respectively. (b) Cartoon illustrating the concept of SMAC method using the *SH* main waves. The method utilizes the interference of *SmS* (left panel) and *sSmS* (right panel) phases in the autocorrelograms. The energy pairs of *SmS* and *sSmS* are enhanced in the autocorrelograms by stacking along the theoretical traveltimes predicted based on epicentral distance x, takeoff angles i_{SmS} (for *SmS*) and i_{sSmS} (for *sSmS*), earthquake depth h and Moho depth H. Earthquake and seismic station are represented by red star and blue triangle, respectively.

with in this paper. The basic concept of SMAC method is to extract the depth phase of an earthquake by autocorrelation and stacking. We first extract the weak depth phase information from the autocorrelograms of the *SH* coda waves and the main *SH* waves; we then further enhance the coherent energy by stacking autocorrelograms over many stations. As the source reflection exhibits different behaviours in the autocorrelograms of coda waves and the main *SH* waves, we formulate the method separately for these two cases.

2.1 SMAC using coda wave

In seismic interferometry, Green's function between two receivers can be obtained by integrating cross-correlations of wavefield observations from an enclosed distribution of sources (Wapenaar & Fokkema 2006). Recently, Curtis *et al.* (2009) showed that Green's function between two subsurface earthquakes could be derived by summing cross-correlograms over an enclosed distribution of receivers by applying reciprocity. In practice, the station distribution could be relaxed to cover the areas of stationary phase. Using seismic coda waves would further relax the requirement of station distribution to extract the Green's functions based on interferometry, as the strong scattering that produces the coda (Aki 1969; Aki & Chouet 1975; Hoshiba 1991; Snieder *et al.* 2002; Campillo 2003) effectively improves the station coverage. Based on this theory, the integration of autocorrelations of seismic coda waves over an enclosed distribution of receivers would represent the Green's function from the earthquake source to the earthquake source, which would contain the two-way travelling seismic energy from the source to the surface and back to the source. We illustrate this concept intuitively in Fig. 1(a). The interference of the scattered waves (e.g. A, B, the left panel) and the surface reflected scattered waves with otherwise same scattering paths (e.g. the counterpart sA, sB, the right panel) would appear at the two-way traveltime between source and the surface in their autocorrelograms, and are enhanced by stacking over many stations. Timing of such emerging energy in the stacked autocorrelograms can be used to estimate the source depth with only the average velocity of the crust needed.

2.2 SMAC using main *SH* waves

When using the main *SH* waves, SMAC explores the interference of the Moho reflections of the down-going wave from a crustal earthquake (*SmS* phase, Fig. 1b) and up-going surface-bounced *SmS* wave (*sSmS* phase, Fig. 1b). These two phases are weak and buried in the other scattered energy in the seismic data. Autocorrelation effectively enhances the energy of these phases because of the similarity of their waveforms, and stacking the autocorrelograms of array data further improves the signal-to-noise (SNR) ratio of the energy. The differential traveltime of *sSmS* and *SmS* places direct constraints on the source depth.

However, the energy of *sSmS* phase with respect to *SmS* energy would appear at different times at different recorded autocorrelograms, and the stacking of the autocorrelograms needs to be following the differential traveltimes between the two phases. The

differential traveltimes $\Delta t = t_{sSmS} - t_{SmS}$ would depend on source depth, epicentral distance, Moho depth and crustal velocity. For a given average crustal shear velocity v:

$$t_{SmS} = \frac{\sqrt{x^2 + (2H - h)^2}}{v}, t_{sSmS} = \frac{\sqrt{x^2 + (2H + h)^2}}{v}, \quad (1)$$

where t_{SmS} and t_{sSmS} are the theoretical traveltimes of *SmS* and *sSmS* phases, respectively, h source depth, H Moho depth and x epicentral distance (Fig. 1b).

We calculate the energy of the stacked autocorrelograms along the theoretical traveltime of Δt for every possible source and Moho depths, assuming an average shear velocity in the crust. We determine the best-fitting source depth to be the depth that generates most prominent energy in the stacked autocorrelograms.

3 SYNTHETIC VALIDATION

3.1 Synthetic test of SMAC using coda wave

We use synthetic examples to demonstrate the validity of the above inferences. In the synthetic test of using coda waves, we construct a model to generate coda waves with distributed random scatterers and compare the depth inference with the model input. The model domain extends 40 km laterally and 40 km in depth. 59 stations are evenly located at the surface within an epicentral distance range from −5.8 km to 5.8 km (Fig. 2a). Source is a vertical dip-slip fault, located at a depth of 1 km. The source time function is a Ricker wavelet with a dominant frequency of 8 Hz. The velocity model consists of 10 000 randomly distributed scatterers with random perturbations from 0 to 30 per cent and randomly varying radii from 0 to 0.2 km (Fig. 2a). The background velocity of the model is 3.5 km s^{-1}. We use 2-D finite difference method to simulate *SH* wave coda. The grid spacing of the finite-difference calculation is 20 m in both horizontal and vertical directions. Absorbing boundary conditions (Clayton & Engquist 1977) are applied on the left, right and bottom boundaries of the finite-difference calculations.

We use the coda seismograms from 2 to 4 s after the direct *SH* waves (Fig. 2b). The autocorrelograms of the coda waves (Fig. 3a) are normalized and stacked. A clear phase, which corresponds to the surface reflection, is visible at $t = \pm 0.56$ s in the stacked autocorrelograms (Fig. 3b). Based on the background velocity of 3.5 km s^{-1}, we obtain a source depth of 0.98 km, with a small error from the model source depth of 1 km. The depth error is due to that the actual average velocity of the model is larger than the background velocity in the presence of strong random scatterers.

3.2 Synthetic test of SMAC using main *SH* wave

In the synthetic test of using main *SH* waves, we test the procedure using a simple two-layer velocity model (Table 1). We use the frequency-wavenumber method of Zhu & Rivera (2002) to calculate theoretical seismograms. The source is a vertical dip-slip fault, located at 10 km depth with a Gaussian source wavelet. 50 stations are distributed surrounding the source, with evenly increasing distances and azimuths (Fig. 4a).

In order to avoid the influence of direct *SH* wave, we do autocorrelation for each waveform from 2 to 30 s after the direct *SH* arrival (Fig. 4b). The search parameter ranges are from 2 to 20 km for source depth h, and 25 to 45 km for Moho depth H. The search grid intervals are 0.1 km for source and Moho depths. The stacked autocorrelogram energy exhibits a concentration of energy near a source depth of 10 km (Fig. 5). From the point of the strongest energy, we obtain a source depth of 10.1 km. Compared to source depth determination, the Moho depth determination has a large error, because of the weak sensitivity of *sSmS–SmS* differential traveltime to the Moho depth.

3.3 Effects of earthquake focal mechanism

In the procedure of using coda wave, we have ignored the effect of earthquake radiation pattern. Coda wave can be divided into two regimes: an earlier diffusion regime and a later equipartitioning

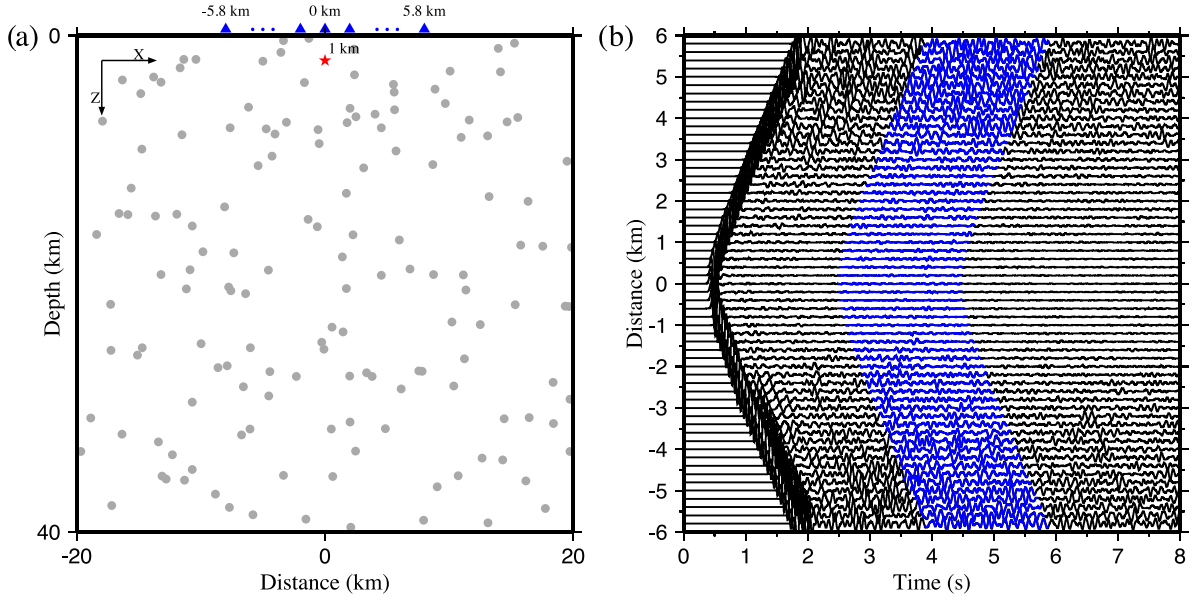

Figure 2. (a) Model of scatterers (grey points) used in 2-D *SH* coda wave synthetics calculation. 59 stations (blue triangles) are evenly distributed on the surface and source (red star) is buried 1 km in depth. Scatterers are randomly distributed with velocity perturbations from 0 to 30 per cent and radii varying from 0 to 0.2 km. The background velocity is 3.5 km s^{-1}. (b) Synthetic seismograms calculated based on the source, model and station configuration in Fig. 2(a). The blue segments of the seismograms are used in the SMAC procedure using *SH* coda waves.

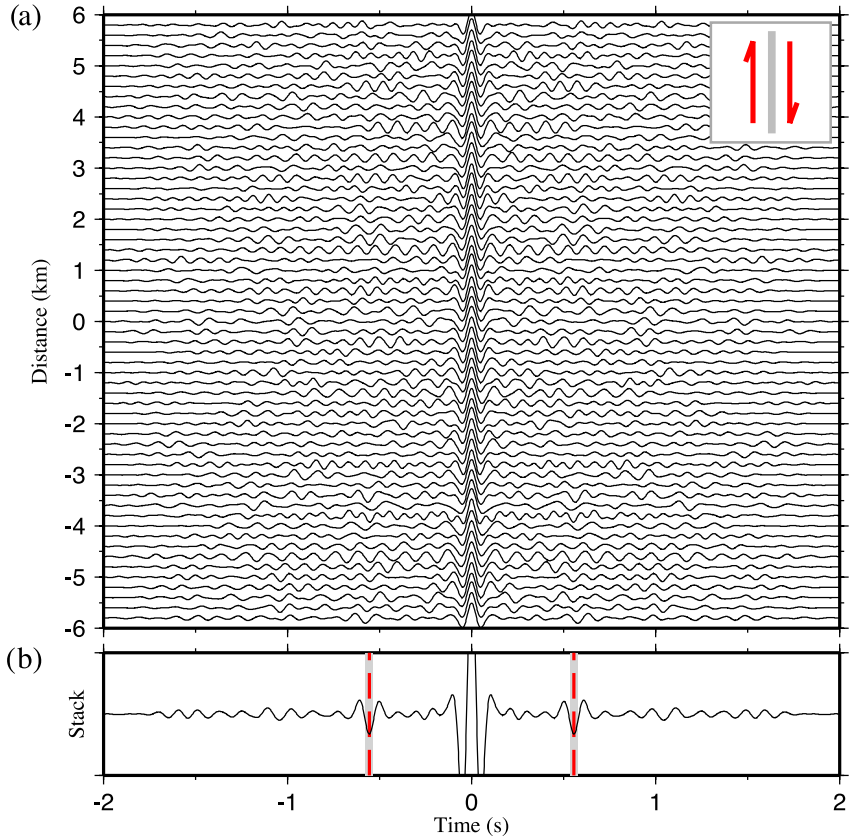

Figure 3. (a) Coda wave autocorrelograms for a vertical dip-slip fault based on the model and station configuration in Fig. 2(a). (b) Autocorrelogram stacked from Fig. 3(a). Two-wave traveltime between the source and the surface is marked by red-dashed lines.

Table 1. Background crustal model used in main *SH* waves synthetic test.

	Depth (km)	V_P (km s^{-1})	V_S (km s^{-1})	Density (g cm^{-3})
Crust	0–35	6.10	3.53	2.81
Upper mantle	35–	8.04	4.47	3.32

regime (Malcolm *et al.* 2004; Yao & van der Hilst 2009). The earlier diffusion part is much stronger, but would depend on earthquake focal mechanism. The later part is more equipartitioned and less sensitive to the focal mechanism, but would usually fall below the ambient noise level. For SMAC applications, the method is most applicable to the faults that radiate strong energy in the vertical

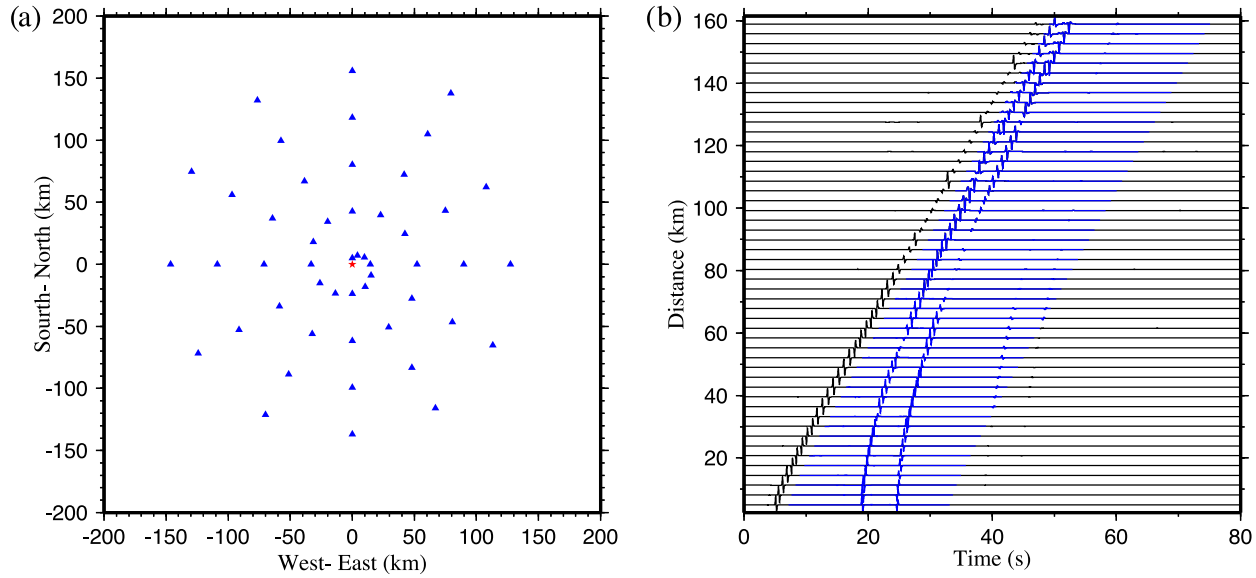

Figure 4. (a) Station distribution used in main *SH* waves synthetic calculations. The source (red star) is buried 10 km in depth, enclosed by 50 stations (blue triangles) with evenly increasing distances and azimuths. (b) Synthetic seismograms calculated based on a two-layered crustal model (Table 1) and station configuration in Fig. 4(a). The blue segments of the seismograms are used in the SMAC procedure using main *SH* waves.

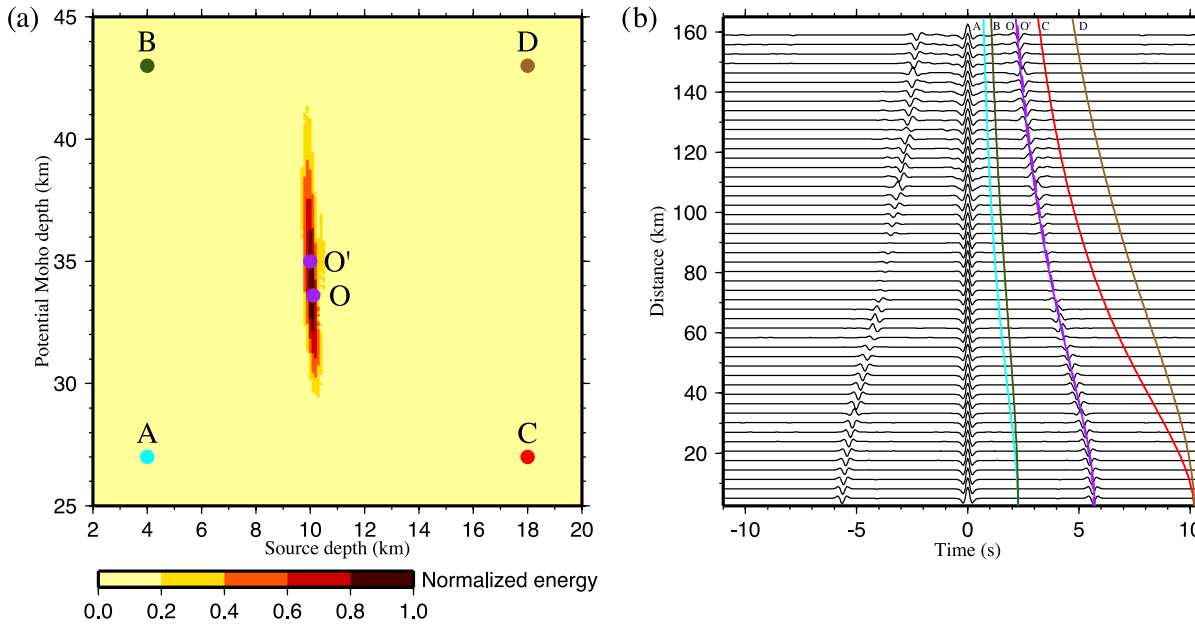

Figure 5. (a) Normalized energy of the autocorrelograms of the main *SH* phases stacked along the predicted traveltime curves based on various source and Moho depths for a dip-slip fault. The source in the synthetic model is located at O′ (10 km, 35 km), while point O (10.1 km, 33.6 km) is the model parameters determined based on its strongest energy. A, B, C and D are example points whose stacking traveltime curves are shown in (b). (b) Autocorrelograms along with six stacking traveltime curves corresponding to model parameters marked as A, B, C, D, O and O′ in (a). Traveltime curves are labelled accordingly. Station distribution is shown in Fig. 4(a).

direction. We would expect that SMAC is most applicable to thrust and normal faults, as the seismic energy radiations of these faults are stronger along the vertical (depth) direction. For these favourable faults, all portions of the coda prove to be equally applicable and produce consistent results (see examples in the real data application later). Synthetics tests confirm such inference. The depth phase is also well recovered for the 45° dip-slip fault (Fig. 6a) as in the case of the vertical dip-slip fault (Fig. 3), but not for the strike-slip fault (Fig. 6b).

In the procedure of using the main *SH* waves, SMAC is able to extract the depth phase for all three fundamental faults (Fig. 5), despite the polarities of the *SmS* and *sSmS* phases could be different at some epicentral distances and azimuths, depending on earthquake focal mechanism. However, if focal mechanism of the earthquake is known, correction can be applied to the autocorrelograms before stacking and stacking results can be further improved. The *SH* wave radiation pattern can be expressed as (eq. 4.86, Aki & Richards 1980):

$$F^{SH} = \cos\lambda\cos\delta\cos i\sin(\phi-\phi_s)+\cos\lambda\sin\delta\sin i\cos 2(\phi-\phi_s) + \sin\lambda\cos 2\delta\cos i\cos(\phi-\phi_s)-\frac{1}{2}\sin\lambda\sin 2\delta\sin i\sin 2(\phi-\phi_s), \quad (2)$$

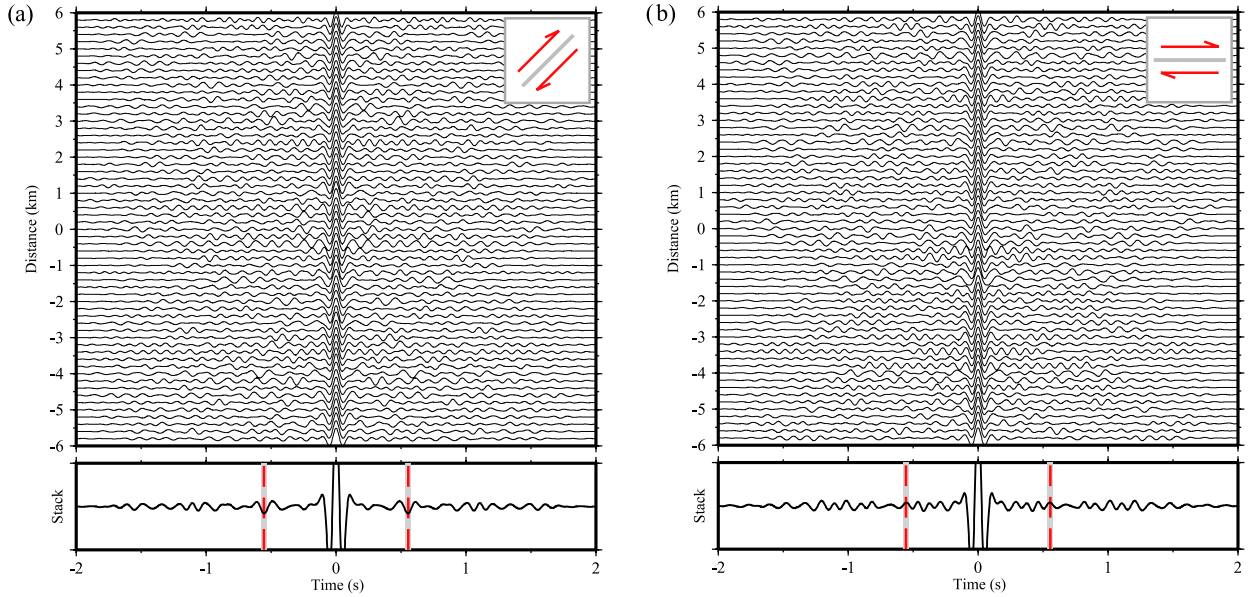

Figure 6. Same as Fig. 3, except that left panel is for a 45° dip-slip fault and right panel for a strike-slip fault.

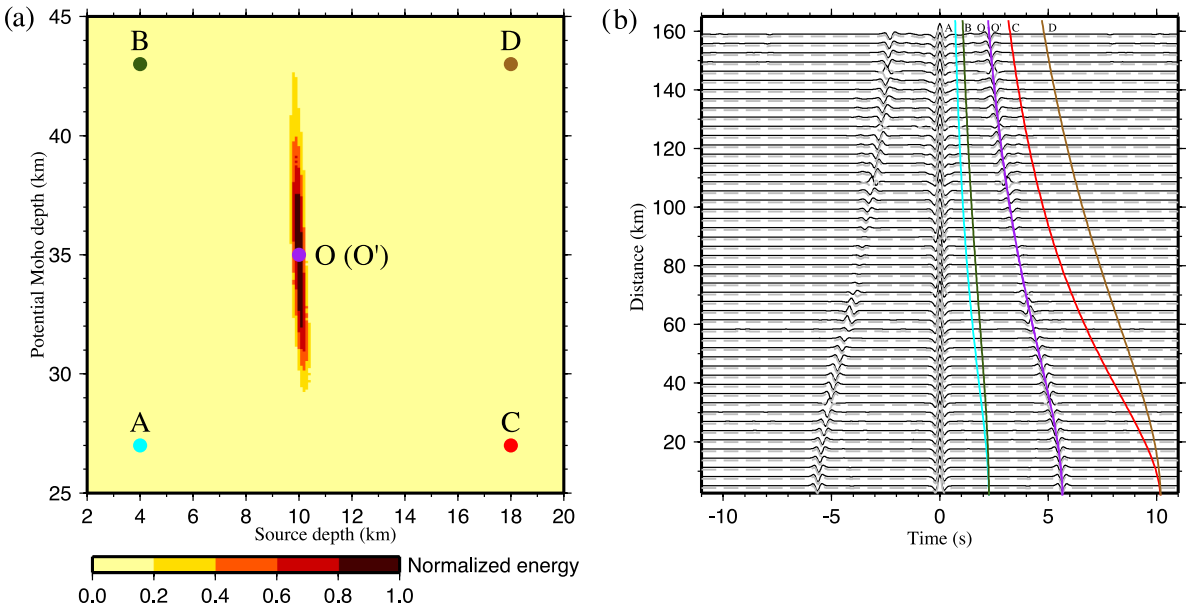

Figure 7. Same as Fig. 5, except that focal mechanism correction is applied. Determined model parameters point O (10.0 km, 35.2 km) is closer to the input point O′ (10.0 km, 35.0 km). The grey-dashed traces represent autocorrelograms flipped based on focal mechanism correction.

where i and ϕ are the take-off angle and station azimuth, respectively, and ϕ_s is the strike, δ is the dip, λ is the rake of the earthquake. The take-off angles of *SmS* and *sSmS* phases can be determined by epicentral distance x, potential Moho depth H and source depth h (Fig. 1b) as follows:

$$i_{SmS} = \arctan\left(\frac{x}{2H-h}\right);\ i_{sSmS} = \pi - \arctan\left(\frac{x}{2H+h}\right). \quad (3)$$

The focal mechanism correction can be applied as such that each autocorrelogram is multiplied by a weight factor, $\varepsilon\sqrt{|F^{SmS}F^{sSmS}|}$, during stacking, where $\varepsilon = 1$ when the radiation patterns of the *SmS* and *sSmS* phases have an opposite sign, and $\varepsilon = -1$ otherwise. Model parameters are better recovered when the focal mechanism correction is applied to the example in Section 3.2 (Fig. 7).

4 SMAC DEPTH DETERMINATION OF AN ACTUAL EARTHQUAKE

As an example, we apply the method to determine the source depth of an earthquake occurring in Japan Island (Fig. 8a). The earthquake occurs at (37.68°N, 139.94°E) based on Japan Meteorological Agency catalogue (Table 2), and is recorded in the high-sensitivity seismograph network (Hi-net), consisting of approximately 800 stations uniformly distributed over the Japan Island, with an average station separation of 20 km. In the following subsections, we present the results of source depth determination of the earthquake using coda waves and main *SH* waves, respectively.

4.1 Determining source depth from coda wave

The recordings of 448 Hi-net stations are chosen for the coda wave analysis within a distance range of 5° from the earthquake. We first convert the observed seismograms to ground velocity by removing the instrument response and then convolve the ground velocity with the short period World-Wide Standardized Seismograph Network instrument response. Coda waves are selected from 30 to 60 s after the first arrivals of the tangential components of the observations, predicted based on IASP91 model (Kennett & Engdahl 1991).

To investigate the effects of the coda waves at different epicentral distances, we divide the stations into five groups at a 1° interval of epicentral distance (Fig. 8a). Autocorrelograms of the coda waves are selected with SNR >1.8 (defined as the ratio of the average energy within a 0.3 s time window centred at the zero lag and the average energy within the neighbouring 1.0 s time window). The selected autocorrelograms are then self-normalized and stacked. The stacked autocorrelograms exhibit a strong phase at about $t = \pm 3.53$ s for every group of stations and for all the stations. The phase is particularly evident in the stacking of the stations in large distances (e.g. 4–5°; Fig. 9b). We speculate that this is because the scattering coda waves are more diffusive at larger distances due to longer paths of scattering. With an average crustal velocity 3.64 km s^{-1} evaluated from the velocity model of Japan Island suggested by Kubo *et al.* (2002), we estimate the source depth of the earthquake to be 6.4 km.

4.2 Determining source depth from main *SH* waves

The main *SH* waves used include tangential seismograms within 130 km from the earthquake. Though with good SNRs, no clear depth phases are discernable in the seismic data (Fig. 8b). The data are converted to the ground velocity and bandpass-filtered in a frequency range of 0.8–8 Hz. 37 autocorrelograms are selected with SNR > 3.6. We follow the processing procedure described in Section 3.2 to determine the source depth of the earthquake. With an average crustal velocity of 3.64 km s^{-1}, we calculate the stacked autocorrelogram energy along the theoretical differential traveltimes for the source depths ranging from 3 to 12 km and the Moho depths from 25 to 45 km. The stacked energy clearly exhibits a maximum value at a source depth of 6.4 km (Fig. 10).

We apply focal mechanism correction during autocorrelogram stacking based on fault parameters provided by National Research Institute for Earth Science and Disaster Prevention (Table 2). Stacked energy is more concentrated at a source depth of 6.5 km after the focal mechanism correction (Fig. 11).

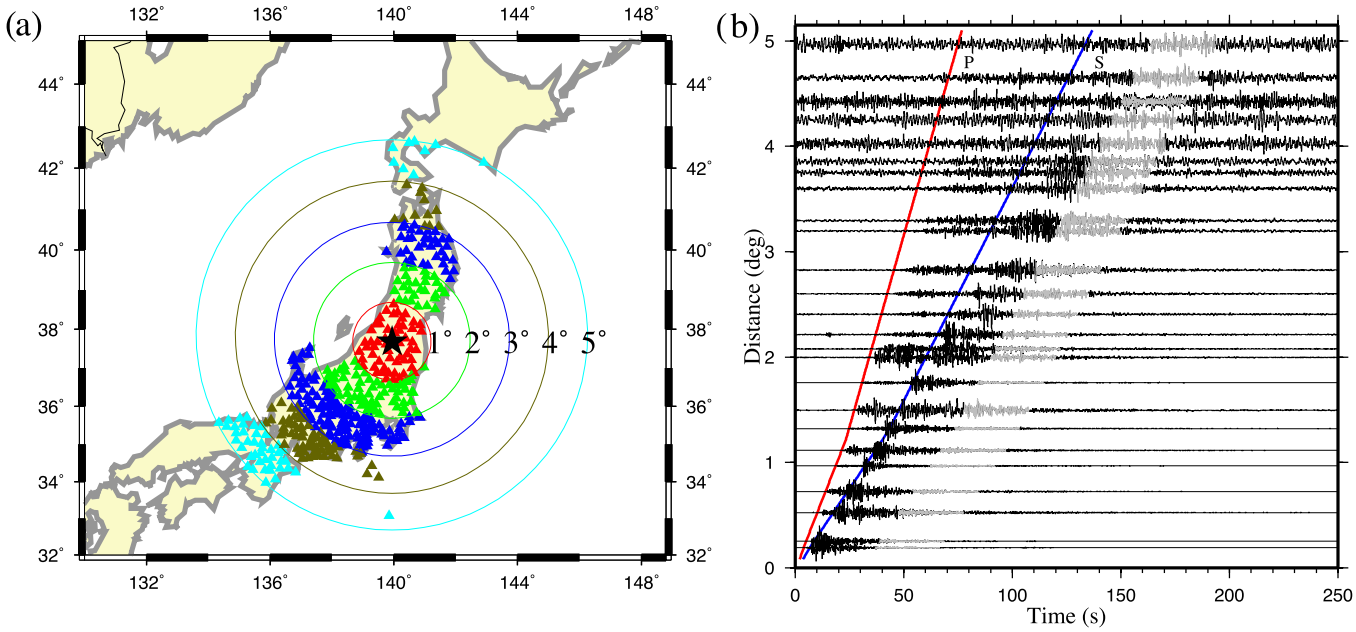

Figure 8. (a) An example of an earthquake (black star, Table 2) occurring in Japan for source depth determination based on the SMAC method and portion of the Hi-net seismic stations (triangles) used. Stations are divided into five groups (colour-coded triangles) within 1° of epicentral distance. Circles mark equal epicentral distance contours. (b) Recorded tangential seismograms at some Hi-net stations, along with theoretical P (red line) and S (blue line) traveltimes. The grey segments of the seismogram are used in the SMAC procedure using *SH* coda waves.

Table 2. Earthquake source parameters.

Origin time (JST)[a]	Latitude[a]	Longitude[a]	Depth[a]	M_w[a]	Strike[b]	Dip[b]	Rake[b]
2011/09/26 14:39:36.73	37.68°N	139.94°E	7.8 km	3.8	86.5°/285.3°	25.1°/66.1°	72.9°/97.8°

[a]Japan Meteorological Agency (JMA).
[b]National Research Institute for Earth Science and Disaster Prevention (NIED).

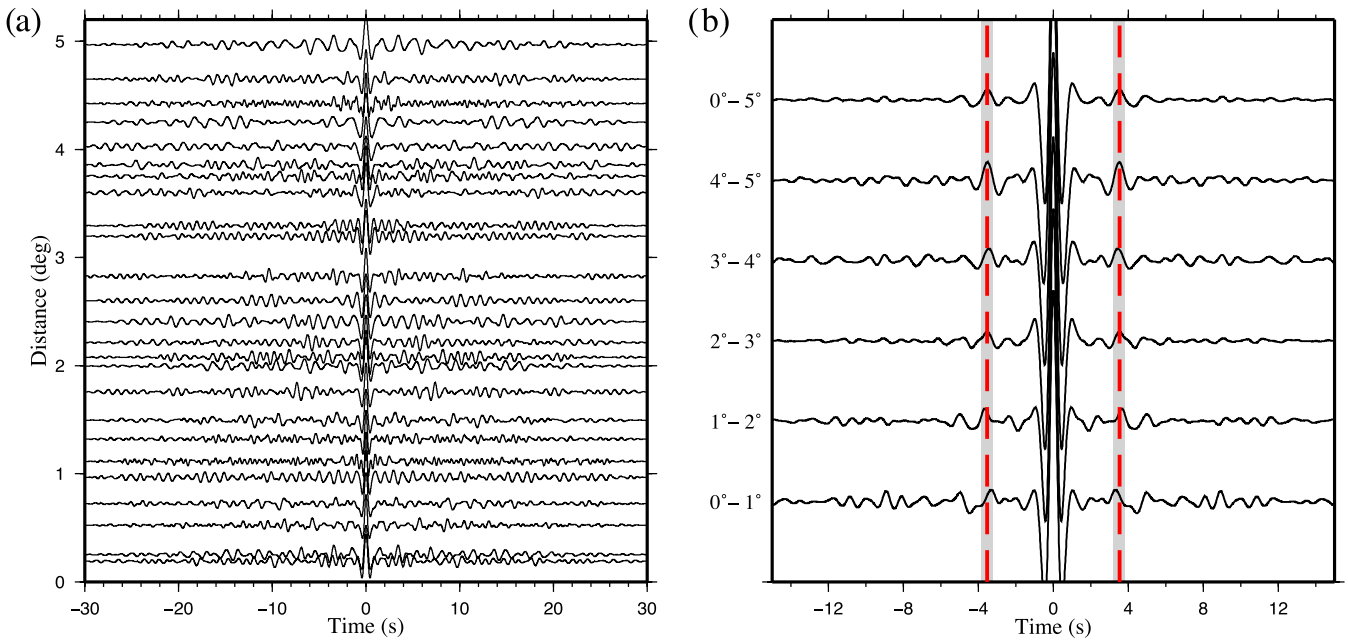

Figure 9. (a) Autocorrelograms of the recorded coda waves in Fig. 8(b). (b) Stacked autocorrelograms for each group of stations defined in Fig. 8(a) (bottom five traces) and for all stations (top trace). Surface reflected phase is marked by red-dashed lines.

5 DISCUSSION

SMAC procedures using both the coda waves and main *SH* waves yield nearly the same result, corroborating each other. The procedures are stable and can also be successfully applied with more limited station coverage and using various time windows of the coda waves (see another example of event depth determination in Supporting Information). The fact that the coda stacks are

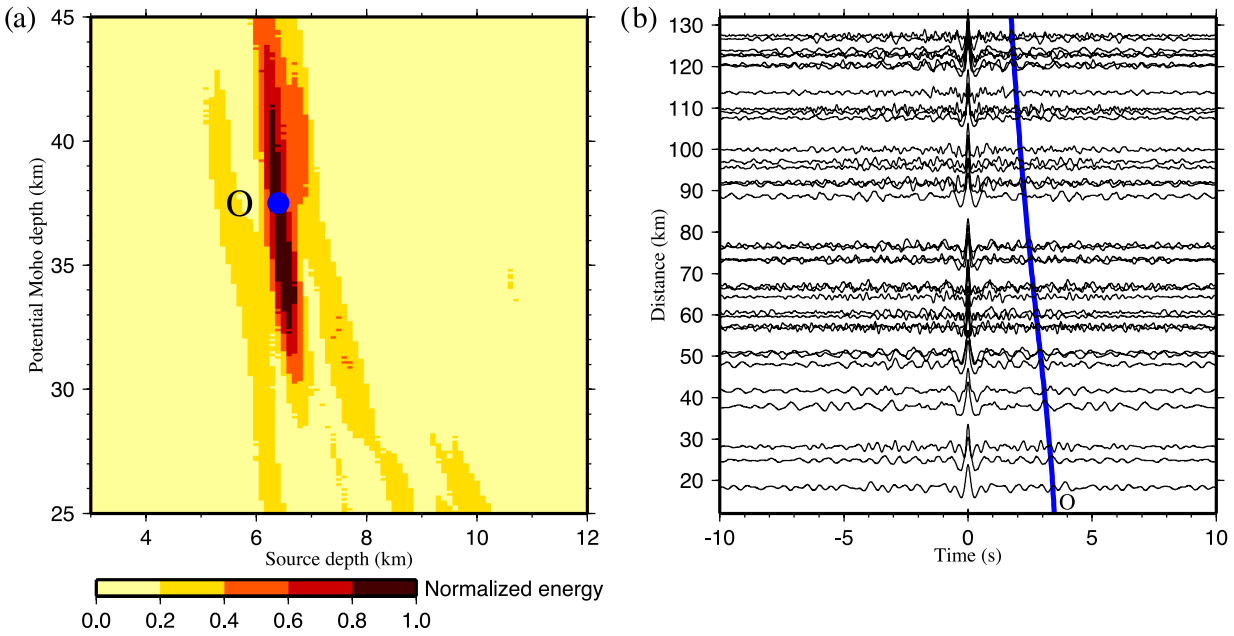

Figure 10. (a) Normalized stacked energy of autocorrelograms of the observed main *SH* waves of the earthquake as a function of source and Moho depths. Point O (6.4 km, 37.5 km), the strongest energy on the map, is picked as the determined parameters. (b) Autocorrelograms used for stacking, along with the traveltime curve (blue line) based on the model parameters of point O in (a).

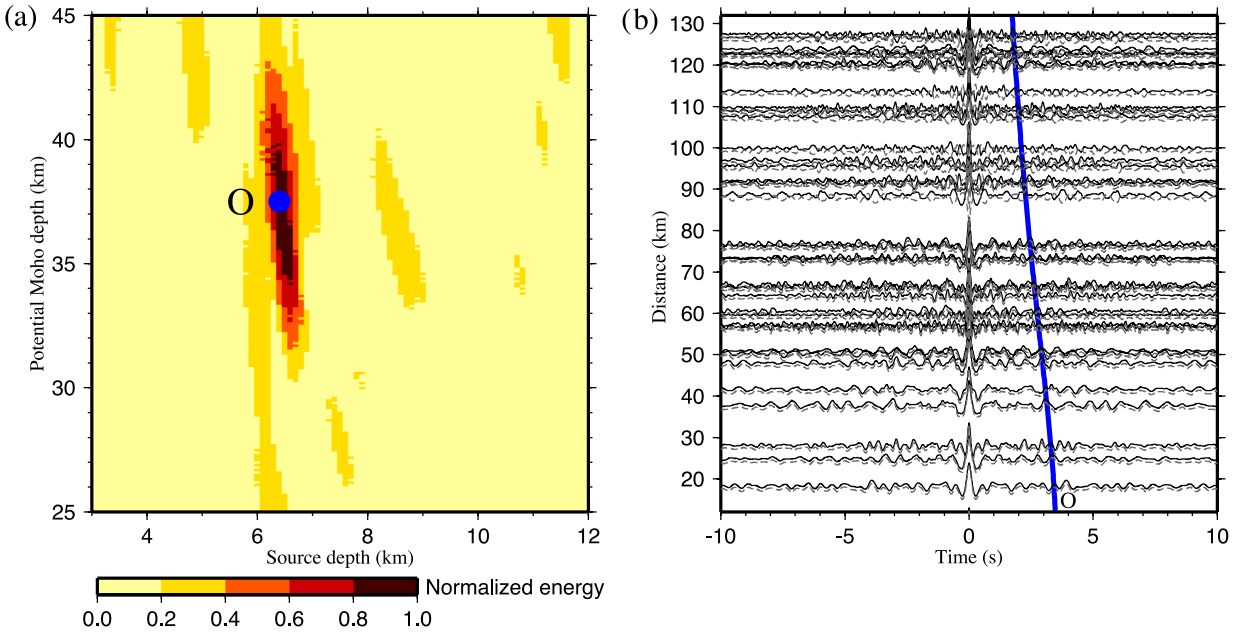

Figure 11. Same as Fig. 10, except that focal mechanism correction is applied. The determined model parameters are located at point O (6.5 km, 36.9 km). Grey-dashed traces (b) represent the autocorrelograms flipped based on focal mechanism correction.

consistent in various time windows (Fig. S2) further supports our assumption that the coda waves are diffusive. The depth inference is weakly dependent on the assumed average crustal velocity. We test a range of assumed average velocity from 3.4 to 3.8 km s^{-1}. The inferred source depth is linearly related to the assumed average crustal velocity in both the coda wave and main *SH* wave analyses (Fig. 12). The inferred source depth changes less than 1 km assuming an uncertainty of 10 per cent in the averaged crust velocity.

In the data application, we find that high-passed filtering with the lowest cut-off frequency in the range of 0.5–1.5 Hz works best when using the *SH* main waves, and the lowest cut-off frequency in the range from 0.4 to 0.8 Hz works best for the coda wave application. Using different lowest cut-off frequencies produces a 0.2 km difference in the source depth determination. At least 15 stations are needed in the coda wave stacking. Beyond that number of the stations, the stacking produces stable and consistent results. We should, however, point out that these parameters would vary with the event and the region of the study. For example, for the smaller earthquake we studied (M_w 3.6, see Supporting Information), the lowest cut-off frequency is from 0.2 to 1.5 Hz for the main *SH* wave analysis and from 0.4 to 0.7 Hz for the coda wave study.

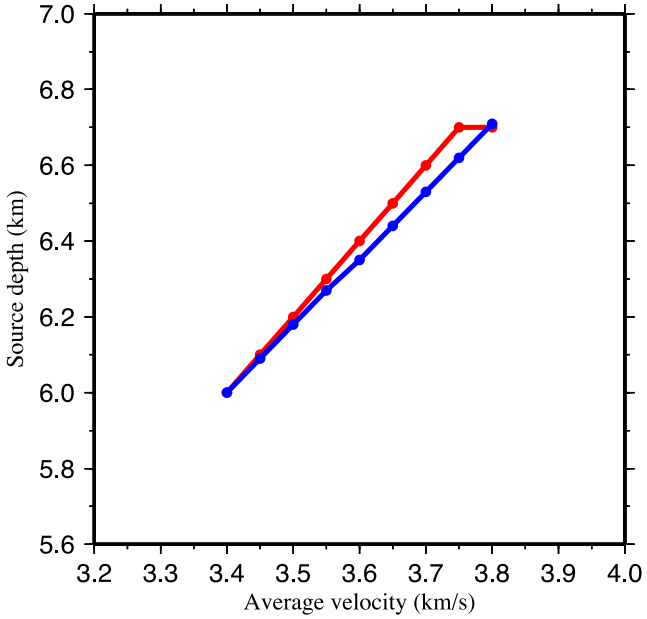

Figure 12. Determined source depth as a function of the average velocity assumed in the coda wave analysis (blue line) and the main *SH* waves analysis (red line). Circles are test points.

While we have employed the interference of *SmS* and *sSmS* pairs to determine the source depth of an earthquake, same concept can also be applied for other purposes using other phase pairs. For example, one can utilize the direct *SH* wave and *sSmS* phase to determine the Moho depth. Two-wave traveltime of the Moho reflections could be extracted from the autocorrelograms energy stacked along the theoretical differential traveltimes of *S* and *sSmS* phases. In fact, the Moho depth (36–37 km) we determined using a simple two-layered crustal model is already close to that determined by Kubo *et al.* (2002) (33 km).

6 CONCLUSIONS

We present a new method to determine earthquake source depth by SMAC using main *SH* waves and their coda waves. The SMAC method extracts the depth phase of an earthquake by autocorrelation and stacking of the *SH* coda and the main *SH* waves, and uses the depth phase information to determine the source depth. In using the coda waves, the stacking of autocorrelations of coda waves represents the Green's function from the earthquake source to itself, which contains the two-way travelling seismic energy from the source to the surface and back to the source. In using the main *SH* waves, SMAC explores the interference of *SmS* and *sSmS* waves. The autocorrelograms of main *SH* waves are stacked along the theoretical differential *sSmS–SmS* traveltime for every possible source and Moho depths, and the source depth is determined at the maximum stacked autocorrelogram energy.

Synthetic tests demonstrate the validity of the SMAC procedures. SMAC method using the coda waves is most applicable to those faults radiating strong energy along the vertical (depth) direction, such as thrust and normal faults, but less suitable for strike-slip faults. In the SMAC procedure of using the main *SH* waves, focal mechanism correction can be applied to further improve the stacking results.

As an example of application, we apply the SMAC method to determine the source depth for an earthquake occurring in Japan Island using main *SH* waves and their coda waves. The stacking of both main *SH* wave and coda autocorrelograms exhibits robust surface reflected energy. Given a reference average crustal velocity 3.64 km s^{-1}, both procedures yield a consistent source depth of 6.4–6.5 km. The estimated depth trades off linearly with the assumed average velocity in the crust. But the error of the depth estimation is less than 1 km assuming an uncertainty of 10 per cent in the averaged crust velocity. Our method offers a new simple way to investigate earthquake source depth in high resolution and the method concept can be extended for other purposes.

ACKNOWLEDGEMENTS

We thank the Hi-net for providing data and Lupei Zhu for sharing his F-K code. This paper benefited significantly from the reviews by Germán Prieto, editor Michael Ritzwoller and an anonymous reviewer. This work was supported by the National Natural Science Foundation of China under Grants NSFC41130311 and the Chinese Academy of Sciences and State Administration of Foreign Experts Affairs International Partnership Program for Creative Research Teams.

REFERENCES

Aki, K., 1969. Analysis of the seismic coda of local earthquakes as scattered waves, *J. geophys. Res.,* **74,** 615–631.

Aki, K. & Chouet, B., 1975. Origin of coda waves: source, attenuation, and scattering effects, *J. geophys. Res.,* **80,** 3322–3342.

Aki, K. & Richards, P.G., 1980. *Quantitative Seismology,* 1st edn, Vol. 1, Freeman, 115 pp.

Billings, S., Kennett, B.L. & Sambridge, M.S., 1994. Hypocentre location: genetic algorithms incorporating problem-specific information, *Geophys. J. Int.,* **118,** 693–706.

Campillo, M., 2003. Long-range correlations in the diffuse seismic coda, *Science,* **299,** 547–549.

Clayton, R. & Engquist, B., 1977. Absorbing boundary conditions for acoustic and elastic wave equations, *Bull. seism. Soc. Am.,* **67,** 1529–1540.

Curtis, A., Nicolson, H., Halliday, D., Trampert, J. & Baptie, B., 2009. Virtual seismometers in the subsurface of the Earth from seismic interferometry, *Nat. Geosci.,* **2,** 700–704.

Hoshiba, M., 1991. Simulation of multiple-scattered coda wave excitation based on the energy conservation law, *Phys. Earth planet. Inter.,* **67,** 123–136.

Kennett, B. & Engdahl, E., 1991. Traveltimes for global earthquake location and phase identification, *Geophys. J. Int.,* **105,** 429–465.

King, R., 1979. Observations of sPn from Swabian Alb earthquakes at the GRF array, *J. Geophys.,* **45,** 337–340.

Kubo, A., Fukuyama, E., Kawai, H. & Nonomura, K.I., 2002. NIED seismic moment tensor catalogue for regional earthquakes around Japan: quality test and application, *Tectonophysics,* **356,** 23–48.

Langston, C.A., 1987. Depth of faulting during the 1968 Meckering, Australia, earthquake sequence determined from waveform analysis of local seismograms, *J. geophys. Res.,* **92,** 11 561–11 511, 11 574.

Lin, G. & Shearer, P., 2005. Tests of relative earthquake location techniques using synthetic data, *J. geophys. Res. Solid Earth* (1978–2012), 110, doi:10.1029/2004JB003380.

Malcolm, A.E., Scales, J.A. & van Tiggelen, B.A., 2004. Extracting the Green function from diffuse, equipartitioned waves, *Physical Rev. E,* **70,** 015601(R)-1–015601(R)-4.

Pavlis, G.L., 1986. Appraising earthquake hypocenter location errors: a complete, practical approach for single-event locations, *Bull. seism. Soc. Am.,* **76,** 1699–1717.

Poupinet, G., Ellsworth, W.L. & Frechet, J., 1984. Monitoring velocity variations in the crust using earthquake doublets: an application to the Calaveras Fault, California, *J. geophys. Res.,* **89,** 5719–5731.

Schaff, D.P. & Richards, P.G., 2004. Repeating seismic events in China, *Science,* **303,** 1176–1178.

Shearer, P., Hauksson, E. & Lin, G., 2005. Southern California hypocenter relocation with waveform cross-correlation, part 2: results using source-specific station terms and cluster analysis, *Bull. seism. Soc. Am.,* **95,** 904–915.

Snieder, R., Grêt, A., Douma, H. & Scales, J., 2002. Coda wave interferometry for estimating nonlinear behavior in seismic velocity, *Science,* **295,** 2253–2255.

Waldhauser, F. & Ellsworth, W.L., 2000. A double-difference earthquake location algorithm: method and application to the northern Hayward fault, California, *Bull. seism. Soc. Am.,* **90,** 1353–1368.

Wapenaar, K. & Fokkema, J., 2006. Green's function representations for seismic interferometry, *Geophysics,* **71,** SI33–SI46.

Wen, L., 2006. Localized temporal change of the Earth's inner core boundary, *Science,* **314,** 967–970.

Yao, H. & van der Hilst, R.D., 2009. Analysis of ambient noise energy distribution and phase velocity bias in ambient noise tomography, with application to SE Tibet, *Geophys. J. Int.,* **179,** 1113–1132.

Zhu, L. & Rivera, L.A., 2002. A note on the dynamic and static displacements from a point source in multilayered media, *Geophys. J. Int.,* **148,** 619–627.

Zonno, G. & Kind, R., 1984. Depth determination of North Italian earthquakes using Grafenberg data, *Bull. seism. Soc. Am.,* **74,** 1645–1659.

SUPPORTING INFORMATION

Additional Supporting Information may be found in the online version of this article:

Figure S1. (a) Another example of an earthquake (black star, Table S1) occurring in Japan for source depth determination based on the SMAC method. Earthquake and portion of the Hi-net seismic stations (triangles, within the epicentral distance range of 3°–4° only) used in coda wave analysis. Circles mark equal epicentral distance contours. (b) Recorded tangential seismograms at some Hi-net stations in (a), along with theoretical P (red line) and S (blue line) traveltimes. Coda segments of the seismograms are colour-marked starting from 15 to 45 s, 30 to 60 s, 45 to 75 s, 60 to 90 s and 75 to 105 s.

Figure S2. (a–c) Some coda wave autocorrelograms in time windows between 15 and 45 s (a), 45 and 75 s (b) and 75 and 105 s (c). (d) Stacked autocorrelograms in various time windows (labelled on the left) and for all time windows (top trace, labelled as 'Stack'). Surface reflected phases are marked by red-dashed lines.

Figure S3. (a) Normalized stacked energy of autocorrelograms of the observed main *SH* waves of the earthquake as a function of source and Moho depths. Point O (6.7 km, 36.0 km), the strongest energy on the map, is picked as the determined parameters. (b) Autocorrelograms used for stacking, along with the traveltime curve (blue line) based on the model parameters of point O in (a). Focal mechanism correction is applied.

Table S1. Earthquake source parameters (http://gji.oxfordjournals.org/lookup/suppl/doi:10.1093/gji/ggu044/-/DC1).